

Supporting Information

Directing the Hetero-Growth of Lattice-Mismatched Surface Mounted Metal–Organic Frameworks by Functionalizing the Interface

Zheng Wang,^a Suttipong Wannapaiboon,^{a,b} Katia Rodewald,^c Min Tu,^d Bernhard Rieger^c and Roland A. Fischer*^a

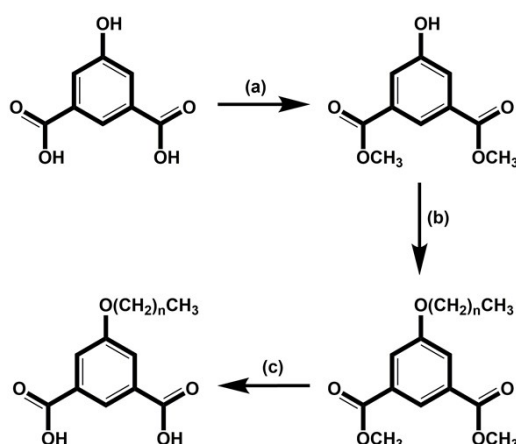
^a Chair of Inorganic and Metal-Organic Chemistry, Department Chemistry & Catalysis Research Center, Technical University of Munich (TUM), D-85748 Garching, Germany

^b Synchrotron Light Research Institute (SLRI), 111 University Avenue, Muang District, 30000 Nakhon Ratchasima, Thailand

^c WACKER-Chair of Macromolecular Chemistry, Department Chemistry & Catalysis Research Center, Technical University of Munich (TUM), D-85748 Garching, Germany

^d Center for Surface Chemistry and Catalysis, Department of Microbial and Molecular Systems, KU Leuven – University of Leuven, Leuven Chem&Tech, Celestijnenlaan200F, Post Box 2461, 3001 Heverlee, Belgium.

Synthesis of fu-ip ligands



(a) methanol, H₂SO₄, reflux 8h;¹ (b) CH₃(CH₂)_nBr, acetone or acetonitrile¹ or N,N-dimethylmethanamide² reflux 16h, n = 0, 1, 2, 3, 5, 9, 17; (c) KOH; methanol; reflux 18h¹

Scheme S1. Synthesis of 5-alkoxyisophthalic acid (fu-ip) linkers.

5-Methoxyisophthalic acid (Me-ip), 5-ethoxyisophthalic acid (Et-ip), 5-propoxyisophthalic acid (Pr-ip) and 5-butoxyisophthalic acid (Bu-ip) were synthesized strictly following the procedures in the literature.¹

5-hexyloxyisophthalic acid (He-ip), 5-decyloxyisophthalic acid (De-ip) and 5-octadecyloxyisophthalic acid (Od-ip) were prepared using the abovementioned protocol as well but altering the solvent to N,N-dimethylmethanamide² in step (b).

In order to synthesize 5-(4-hydroxybutoxy)isophthalic acid (BuOH-ip), we firstly prepared 4-bromo-1-butanol by adding concentrated H₂SO₄ and HBr dropwise to THF at 0 °C with stirring and refluxing for 90 min, and used it as precursor.³ Then 4-bromo-1-butanol was reacted with dimethyl 5-hydroxyisophthalate to form dimethyl 5-(4-hydroxybutoxy)isophthalate. After that, the obtained chemical was hydrolyzed and acidified to form the desired organic linkers BuOH-ip.

NMR characterization of fu-ip ligands

Me-ip: ¹H NMR (400 MHz, DMSO-*d*₆) δ 13.31 (bs, 2H, -CO₂H), 8.08 (t, 1H, Ar-H, *J* = 3 Hz), 7.65 (d, 2H, Ar-H, *J* = 1.44 Hz), 3.87 (s, 3H, -CH₃). ¹³C NMR (101 MHz, DMSO-*d*₆) δ 166.87 (-CO₂H), 159.85 (C-OMe), 133.07 (C-CO₂H), 122.67 (Ar), 119.00 (Ar), 56.12 (-CH₃) ppm.

Et-ip: ¹H (400 MHz, DMSO-*d*₆) δ 13.29 (bs, 2H, -CO₂H), 8.07 (t, 1H, Ar-H, *J* = 2.93 Hz), 7.63 (d, 2H, Ar-H, *J* = 1.47 Hz), 4.13 (q, 2H, -CH₂CH₃, *J* = 20.8 Hz). 1.36 (t, 3H, -CH₃, *J* = 13.8 Hz). ¹³C NMR (101 MHz, DMSO-*d*₆) δ 166.89 (-CO₂H), 159.11 (C-OEt), 133.06 (C-CO₂H), 122.56 (Ar), 119.44 (Ar), 64.22 (-CH₂CH₃), 14.95 (-CH₃) ppm.

Pr-ip: ¹H (400 MHz, DMSO-*d*₆) δ 13.28 (bs, 2H, -CO₂H), 8.07 (t, 1H, Ar-H, *J* = 5.28 Hz), 7.63 (d, 2H, Ar-H, *J* = 1.32 Hz), 4.04 (t, 2H, -OCH₂-, *J* = 35.2 Hz), 1.75 (m, 2H, -CH₂CH₃), 1.00 (t, 3H, -CH₃, *J* = 14.8 Hz). ¹³C NMR (101 MHz, DMSO-*d*₆) δ 166.89 (-CO₂H), 159.27 (C-OPr), 133.05 (C-CO₂H), 122.56 (Ar), 119.47 (Ar), 70.01 (-OCH₂-), 22.37 (-CH₂CH₃), 10.76 (-CH₃) ppm.

Bu-ip: ¹H NMR (400 MHz, DMSO-*d*₆) δ 13.28 (bs, 2H, -CO₂H), 8.07 (t, 1H, Ar-H, *J* = 2.96 Hz), 7.63 (d, 2H, Ar-H, *J* = 1.44 Hz), 4.07 (m, 2H, -OCH₂-), 1.72 (m, 2H, -CH₂CH₂CH₃), 1.44 (m, 2H, -CH₂CH₃), 0.94 (t, 3H, -CH₃, *J* = 18.7 Hz). ¹³C NMR (101 MHz, DMSO-*d*₆) δ 166.89 (-CO₂H), 159.26 (C-OBu), 133.03 (C-CO₂H), 122.57 (Ar), 119.45 (Ar), 68.25(-OCH₂-), 31.03 (-CH₂CH₂CH₃), 19.10 (-CH₂CH₃), 14.12 (-CH₃) ppm.

He-ip: ¹H NMR (400 MHz, DMSO-*d*₆) δ 13.27 (bs, 2H, -CO₂H), 8.07 (t, 1H, Ar-H, *J* = 2.92 Hz), 7.63 (d, 2H, Ar-H, *J* = 1.85 Hz), 4.06 (t, 2H, -OCH₂-, *J* = 12.8 Hz), 1.73 (m, 2H, -CH₂(CH₂)₃CH₃), 1.42 (m, 2H, -CH₂(CH₂)₂CH₃), 1.31 (m, 4H, -(CH₂)₂CH₃), 0.87 (q, 3H, -CH₃, *J* = 13.8 Hz). ¹³C NMR (101 MHz, DMSO-*d*₆) δ 166.88 (-CO₂H), 159.26 (C-OHe), 133.04 (C-CO₂H), 122.56 (Ar), 119.45 (Ar), 68.53 (-OCH₂-), 31.42 (-CH₂(CH₂)₃CH₃), 28.93 (-CH₂(CH₂)₂CH₃), 25.53 (-CH₂CH₂CH₃), 22.52 (-CH₂CH₃), 14.34 (-CH₃) ppm.

De-ip: ^1H NMR (400 MHz, $\text{DMSO-}d_6$) δ 13.27 (bs, 2H, $-\text{CO}_2\text{H}$), 8.07 (t, 1H, Ar-H, $J = 3.16$ Hz), 7.62 (d, 2H, Ar-H, $J = 1.48$ Hz), 4.06 (t, 2H, $-\text{OCH}_2-$, $J = 12$ Hz), 1.72 (m, 2H, $-\text{CH}_2(\text{CH}_2)_7\text{CH}_3$), 1.41 (m, 2H, $-\text{CH}_2(\text{CH}_2)_6\text{CH}_3$), 1.23 (m, 12H, $-(\text{CH}_2)_6\text{CH}_3$), 0.84 (t, 3H, $-\text{CH}_3$, $J = 13.4$ Hz). ^{13}C NMR (101 MHz, $\text{DMSO-}d_6$) δ 166.89 ($-\text{CO}_2\text{H}$), 159.24 (C-ODE), 133.07 (C- CO_2H), 122.57 (Ar), 119.43 (Ar), 68.51 ($-\text{OCH}_2-$), 31.76 ($-\text{CH}_2(\text{CH}_2)_7\text{CH}_3$), 29.45-28.95 (5C, $-(\text{CH}_2)_5(\text{CH}_2)_2\text{CH}_3$), 25.84 ($-\text{CH}_2\text{CH}_2\text{CH}_3$), 22.56 ($-\text{CH}_2\text{CH}_3$), 14.39 ($-\text{CH}_3$) ppm.

Od-ip: ^1H NMR (400 MHz, $\text{DMSO-}d_6$) δ 13.27 (bs, 2H, $-\text{CO}_2\text{H}$), 8.07 (t, 1H, Ar-H, $J = 3.08$ Hz), 7.63 (d, 2H, Ar-H, $J = 1.84$ Hz), 4.06 (t, 2H, $-\text{OCH}_2-$, $J = 12.8$ Hz), 1.73 (m, 2H, $-\text{CH}_2(\text{CH}_2)_{15}\text{CH}_3$), 1.42 (t, 2H, $-\text{CH}_2(\text{CH}_2)_{14}\text{CH}_3$, $J = 15.2$ Hz), 1.23 (m, 28H, $-(\text{CH}_2)_{14}\text{CH}_3$), 0.85 (t, 3H, $-\text{CH}_3$, $J = 49.2$ Hz). ^{13}C NMR (101 MHz, $\text{DMSO-}d_6$) δ 166.88 ($-\text{CO}_2\text{H}$), 159.25 (C-OOD), 133.05 (C- CO_2H), 122.57 (Ar), 119.44 (Ar), 68.51 ($-\text{OCH}_2-$), 31.77 ($-\text{CH}_2(\text{CH}_2)_{15}\text{CH}_3$), 29.51-28.96 (13C, $-(\text{CH}_2)_{13}(\text{CH}_2)_2\text{CH}_3$), 25.83 ($-\text{CH}_2\text{CH}_2\text{CH}_3$), 22.56 ($-\text{CH}_2\text{CH}_3$), 14.40 ($-\text{CH}_3$) ppm.

BuOH-ip: ^1H NMR (400 MHz, $\text{DMSO-}d_6$) δ 13.28 (bs, 2H, $-\text{CO}_2\text{H}$), 8.07 (m, 1H, Ar-H), 7.65 (q, 2H, Ar-H, $J = 7.6$ Hz), 4.17 (m, 2H, $-\text{OCH}_2-$, $J = 7.6$ Hz), 3.44 (m, 2H, $-\text{CH}_2\text{OH}$), 1.93 (m, 2H, $-\text{CH}_2\text{CH}_2\text{CH}_2\text{OH}$), 1.51-1.79 (m, 2H, $-\text{CH}_2\text{CH}_2\text{OH}$). ^{13}C NMR (101 MHz, $\text{DMSO-}d_6$) δ 166.89 ($-\text{CO}_2\text{H}$), 159.22 (C-OBuOH), 133.07 (C- CO_2H), 122.63 (Ar), 119.50 (Ar), 70.07 ($-\text{OCH}_2-$), 68.17 ($-\text{CH}_2\text{OH}$), 26.03 ($-\text{CH}_2\text{CH}_2\text{CH}_2\text{OH}$), 25.62 ($-\text{CH}_2\text{CH}_2\text{OH}$) ppm.

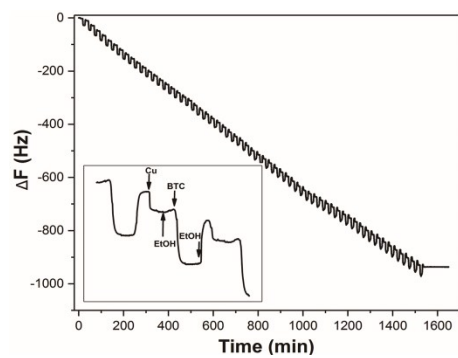


Fig. S1 QCM frequency as a function of time recorded in situ during the stepwise liquid phase epitaxial growth of surface mounted metal-organic framework Cu_3btc_2 (SURMOF **B**, btc = 1,3,5-benzenetricarboxylate, 60 cycles) on the carboxylate-terminated Au covered QCM substrate. Inset: QCM profile of deposition step.

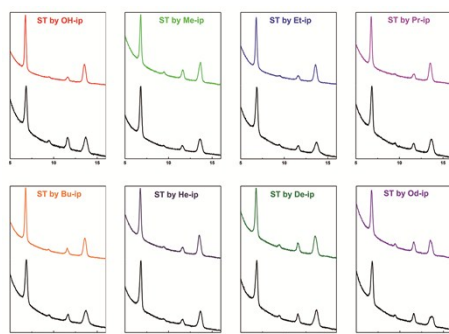


Fig. S2 The comparison of out-of-plane XRD patterns of SURMOF **B** before (black curve) and after (color curve) the implementation of fu-ip ligands on its external surface. The term ST abbreviates surface termination, and OH-ip represents 5-hydroxyisophthalic acid.

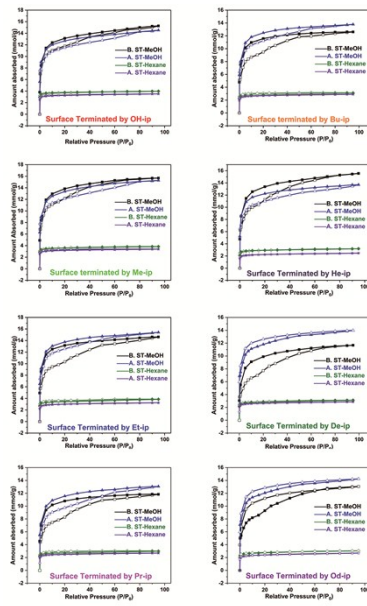


Fig. S3 The comparison of methanol and *n*-hexane sorption isotherms of SURMOF **B** before and after the implementation of fu-ip ligands on its external surface. Adsorption and desorption are labelled with the hollow symbols and solid symbols, respectively. Herein, B. ST represents “before surface termination” and A. ST means “after surface termination”.

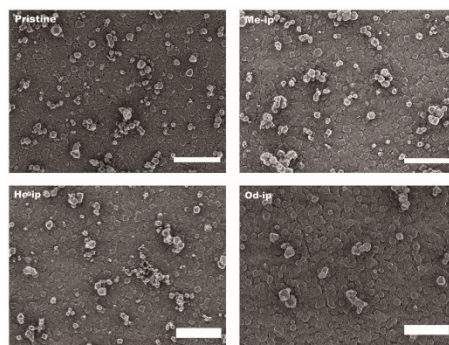


Fig. S4 Scanning electron microscopic (SEM) images of the pristine SURMOF **B** and the SURMOF **B** samples after the implementation of fu-ip ligands on their external surface. Here, the samples with the Me-ip, He-ip and Od-ip surface termination were selected for comparison with the pristine SURMOF **B**. Note that the scale bar in the SEM images represents a size of 1 μm .

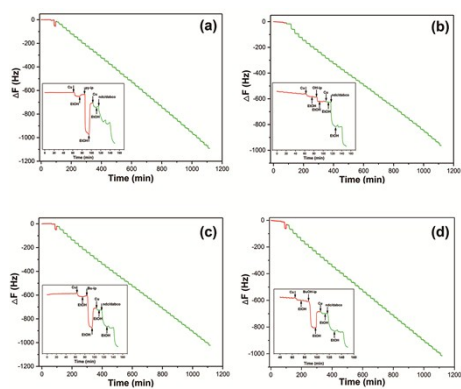


Fig. S5 QCM frequency as a function of time recorded in situ during the stepwise liquid phase epitaxial growth of SURMOF $\text{Cu}_2\text{ndc}_2\text{dabco}$ (**A**, 40 cycles) on the top of the preformed, surface-functionalized SURMOF **B**. In this case, the interface between the two SURMOFs was functionalized by (a) py-ip, (b) OH-ip, (c) Bu-ip, (d) BuOH-ip. Inset: QCM profile during the deposition steps of $\text{Cu(OAc)}_2/\text{fu-ip}$ (red) and SURMOF **A** (green).

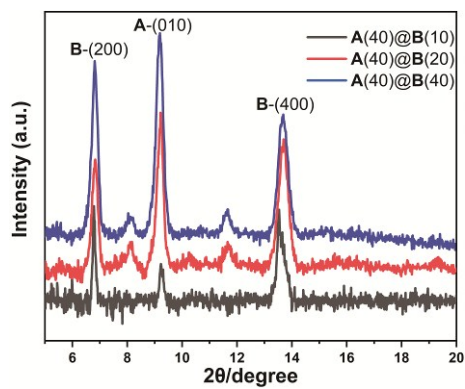


Fig. S6 The comparison of out-of-plane XRD patterns of hetero-SURMOF **A@B** in which 40 cycles SURMOF **A** on SURMOF **B** with different thickness (black: 10 cycles, red: 20 cycles and blue: 40 cycles). The interface between SURMOF **A** and **B** was functionalized with BuOH-ip. For clarity, 40 cycles SURMOF **A** deposited on 10-cycles SURMOF **B** abbreviates to **A(40)@B(10)** and the others are similar. Herein, **B-(200)** stands for (200) XRD peak of SURMOF **B** and the rest are the same.

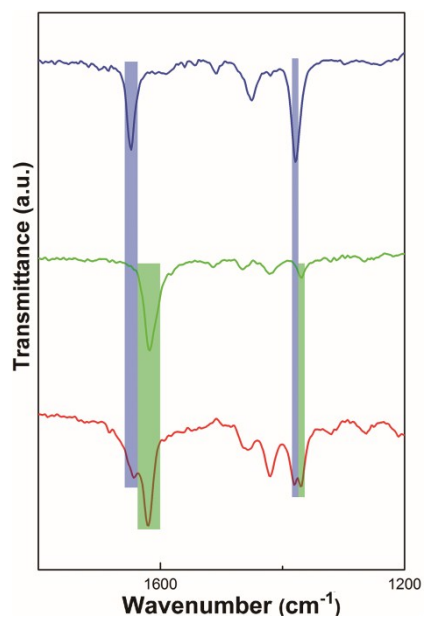


Fig. S7 Infrared reflection absorption spectroscopy (IRRAS) spectra of SURMOF **B** (blue), SURMOF **A** (green) and hetero-SURMOF **A@B** (red). As demonstration, the hetero-SURMOF **A@B** generally reveals a combination of the IR bands between the single components of SURMOF **A** and **B**, highlighting the existence of both components within the hetero-SURMOF.

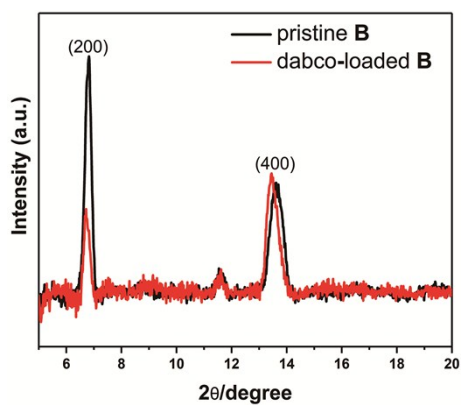


Fig. S8 The comparison of out-of-plane XRD patterns of pristine SURMOF **B** (black curve) and after the loading of dabco molecules (red curve). After loading, the intensity ratio of (200)/(400) are decreased.

References

1. L. J. McCormick, S. A. Morris, A. M. Z. Slawin, S. J. Teat and R. E. Morris, *Cryst. Growth Des.*, 2016, **16**, 5771.
2. V. Berl, I. Huc, J.-M. Lehn, A. DeCian and J. Fischer, *Eur. J. Org. Chem.*, 1999, 3089.
3. J.-T. Nguyen, C.-A. McEwen and E. E. Knaus, *Drug Develop. Res.*, 2000, **51**, 233.